

Direct Solution-Chemical-Bonding Observations by High-Resolution X-Ray Fluorescence Spectroscopy

Tom Scimeca⁽¹⁾ and Yohichi Gohshi⁽²⁾

⁽¹⁾*NTT Interdisciplinary Research Laboratories, Musashino-shi, Tokyo 180, Japan*

⁽²⁾*Department of Industrial Chemistry, Faculty of Engineering, University of Tokyo, Hongo, Bunkyo-ku, Tokyo 113, Japan*

(Received 30 July 1991)

An investigation of solutions by high-resolution x-ray fluorescence spectroscopy has been performed on chloride and sulfide solutions. In this study, dramatic Cl $K\beta$ and $K\alpha$ spectral changes are observed when NaCl(s) is dissolved in water. These spectral changes are interpreted on the basis of chemically dependent x-ray shakeoff satellites. Aqueous sulfide measurements were also performed indicating that, in contrast to Cl, a S-H σ bond was observed about 3.5 eV below the S lone pair peak.

PACS numbers: 82.80.Ej, 78.70.En

While there have been numerous high-resolution x-ray fluorescence spectroscopy (HRXRFS) studies on both solids and gases [1], there have been only a few studies on liquids. These studies have focused primarily on liquid metals [2-4] and liquid Si at elevated temperatures [5]. There has been, up to now, only one HRXRFS study of a solid dissolved in solution [6]. Unfortunately, no solution-chemical-bonding-related spectral changes were reported in that study.

In this Letter, we report significant spectral changes as NaCl(s) and Na₂S are dissolved in water. This is the first time high-resolution x-ray fluorescence spectral differences have been reported, to the best of our knowledge, for a solid as it exists in the solid state and as it exists dissolved in solution. Distinct chemical-bonding differences have also been observed between the Cl⁻ and S²⁻ anions and attributed to differences in the anion-to-hydrogen chemical-bond strength.

Several unique attributes make HRXRFS particularly suited as a solution-chemical-bonding tool. The first concerns the atomlike character of the core state. This quality eliminates initial-final-state effects since the core state is insensitive to valence chemical-bonding effects [7]. Furthermore, x-ray fluorescence spectra provide a measure of the angular-momentum-selected partial density of states localized around the core hole. This is of importance since the atom of interest is most likely a minority species in solution. Furthermore, since XRF is a bulk probe, surface contamination effects play a very minor role, provided the measurement is made at a normal geometry. Finally, since x-ray fluorescence is a "photon in-photon out" technique, measurement of liquids can be performed in either He or air (provided the photon energy is greater than ≈ 600 eV).

In addition to providing a picture of the intrinsic partial density of states, multiple-ionization satellites are also observed when the incident radiation energy sufficiently exceeds the core hole binding energy [8-10]. While these multiple-ionization satellites can complicate spectral interpretation, they provide chemical-bonding information as well [11].

Liquids and solutions have been investigated at the molecular level by both structural and chemical-bonding

probes. Commonly used structural tools include x-ray and neutron diffraction (XRD, ND) [12] as well as more localized structural probes such as extended x-ray-absorption fine-structure spectroscopy (EXAFS) [13] and anomalous dispersion x-ray diffraction (ADXRD) [14]. While these structural tools have been used with a great deal of success in studying liquids and solutions, valence electron chemical-bonding tools have been used far less frequently and with not as much success. Photoelectron spectroscopy has been used with great ingenuity to provide a variety of information on solutions [15]. Yet, this technique poses rather strict differential pumping requirements. Furthermore, information is rather surface sensitive and in the case of valence band spectroscopy, not very selective. X-ray-absorption near-edge fine structure (XANES) has the limitation that only the unoccupied states are probed. Interpretation of bonding changes in the occupied valence band of UV-visible spectra can be complicated due to the "initial-final-state" problem. Thus the motivation of this work is to show that HRXRFS can be used to provide information on the valence band partial density of states of a minority species selectively in an aqueous solution.

The HRXRFS measurements were performed on a Rigaku double crystal instrument that has been described elsewhere [16]. A Sc x-ray tube (50 kV, 50 mA) was used as the excitation source with two Ge(111) crystals in the θ, θ arrangement to disperse the fluorescence radiation. All measurements presented here were made in He at atmospheric pressure. The spectra presented here are the result of added individual spectrum to improve the signal-to-noise ratio and finally numerically smoothed [17].

In Fig. 1, the Cl $K\beta$ (Cl $1s^{-1}3p^{-1}$) spectra are plotted for NaCl(s), Cl⁻(aq), ClO₄⁻(aq), and NH₄Cl(s). The first point to be made is the large spectral differences between NaCl(s) and Cl⁻(aq). This is, to our belief, the first time solid-solution HRXRFS spectral changes have been observed. In particular, large differences are observed on the high-energy side of the main Cl $K\beta_1$ peak.

To understand these spectral differences, it is important to note that the high-energy region in the Cl $K\beta$ spectra has been ascribed to multiple-ionization transi-

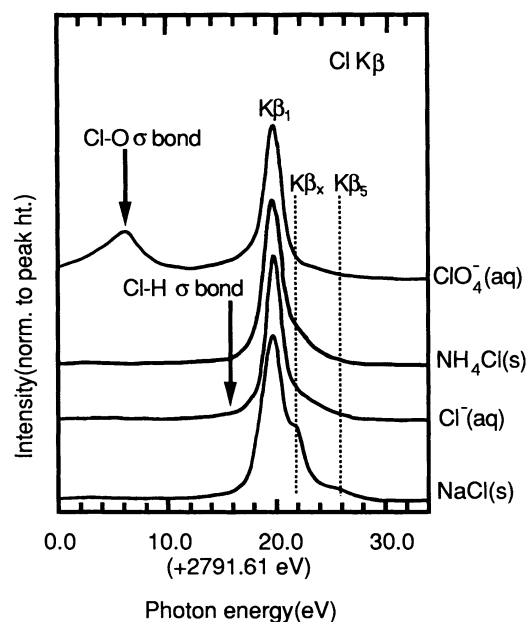


FIG. 1. The CL $K\beta$ spectra are plotted for NaCl(s), Cl^- (aq), ClO_4^- (aq), and NH_4Cl (s), where the relatively narrow spectra corresponds to Cl^- (aq). The main peak (Cl $K\beta_1$) is assigned to a $1s^{-1}$ -(lone pair) $^{-1}$ one-electron transition. The two high-energy peaks Cl $K\beta_x$ and Cl $K\beta_5$ are attributed to multiple-ionization satellites, as discussed in the text. The ClO_4^- (aq) Cl $K\beta$ spectra were shifted by approximately 3.6 eV to put the spectra in line with the Cl^- spectra.

tions [12,18,19]. In particular, while the Cl $K\beta$ peak is assigned to a Cl $1s^{-1}$ -(lone pair) $^{-1}$ one-electron transition, $K\beta_x$ has been assigned to a Cl $1s^{-1}3s^{-1}3s^{-1}3p^{-1}$ electron transition and the $K\beta_5$ peak to a Cl $1s^{-1}3p^{-2}3p^{-3}$ multiply excited electron transition [13,20]. What is of interest here is not the detailed nature of these x-ray satellites so much as an understanding behind the x-ray satellite intensity differences among NaCl(s), Cl^- (aq), and ClO_4^- (aq) [21]. To this end, first consider that the Cl nearest-neighbor changes from Na^+ to H as NaCl(s) is dissolved in water, and that the nature of the Cl nearest-neighbor bond changes from being very ionic to one that is somewhat covalent. The multiple-ionization (shakeoff) probability has been worked out by Åberg [22] in the sudden approximation and is given by

$$P = 6(1 - \langle \psi | \psi^* \rangle^2) / \langle \psi | \psi^* \rangle^2, \quad (1)$$

where ψ^* and ψ are the relaxed and unrelaxed wave functions associated with shakeoff, respectively. One would expect a larger relaxation for an ionic species since the valence electrons are more localized around the generated core hole. Thus, for an ionic species, the orbital overlap term is small and P , the shakeoff probability is large. This is confirmed by the high intensity in the high-energy region for the NaCl Cl $K\beta$ spectra and the low intensity in the high-energy region for the very co-

valent ClO_4^- anion. The high-energy satellite intensity for Cl^- (aq) lies somewhere between NaCl(s) and ClO_4^- (aq). Therefore, we interpret the spectral differences between NaCl(s) and Cl^- (aq) on the high-energy side of the Cl $K\beta_1$ peak as being due to chemical-bonding-dependent multiple-ionization satellites.

This interpretation is also confirmed by the electronegativity differences between Cl and its nearest neighbor as shown in Table I [23]. Further, increases in the ionicity of the Cl nearest-neighbor bond correlate well with the high-energy satellite intensity. Discrete-variational (DV) $X\alpha$ cluster calculations [24] were also performed in order to calculate the relative relaxation energies of the valence lone pair orbital in response to the generation of the Cl $1s$ core hole. This relaxation energy should be related to the overlap between the relaxed and unrelaxed orbital involved in the shakeoff process and provide an indication of the shakeoff probability [25-27]. The DV- $X\alpha$ relaxation energy calculation results are also shown in Table I. It is evident in this table that the absolute relaxation energy is not satisfactory inasmuch as the ClO_4^- relaxation energy exceeds the relaxation energy of Cl^- (aq). The high-energy relaxation is in contrast to the small satellite intensity on the high-energy side of the ClO_4^- Cl $K\beta$ main peak relative to Cl^- (aq). However, if the Cl valence molecular orbital involved in the multiple electron transition is corrected by subtracting the Cl relaxation energy of the nearest-neighbor relaxation energy (nearest-neighbor valence molecular orbital), one observes a much more physically reasonable correlation in that the relative Cl $1s$ core-hole-induced relaxation is greatest for the Cl-Na ionic bond and smallest for the very covalent Cl-O bond.

Finally, a measurement was performed on NH_4Cl (s) since the Cl nearest neighbor for NH_4Cl (s) is H, just as it is for Cl^- (aq). Although solid-state broadening is estimated at 1.2 eV, the intensity on the high-energy side of the Cl $K\beta$ main peak for NH_4Cl (s) is quite similar to Cl^- (aq) indicating that Cl nearest-neighbor localization determines to a large degree the shakeoff probability and hence the high-energy satellite intensity in the Cl $K\beta$ spectra.

TABLE I. A number of useful parameters are listed for the three Cl nearest-neighbor bonds. Pauling electronegativity differences (Cl nearest neighbor) are listed in the first column while the remaining columns concern theoretical relaxation energies (DV- $X\alpha$) following the creation of a Cl $1s$ core hole.

Cluster	$\Delta\chi^a$	Relaxation energy (eV)		
		Cl	nn	Cl-nn (ΔE_R)
ClNa_6^{5+}	2.23	11.73	5.81	5.92
$\text{Cl}(\text{H}_2\text{O})_6^-$	0.96	7.25	4.67	2.58
ClO_4^-	0.28	8.67	8.56	0.11

^aElectronegativity values, see Ref. [23].

Another noteworthy aspect of the Cl^- (aq) spectra is the absence of any strong Cl-H bonding. Gilberg has measured the Cl $K\beta$ spectra of HCl [28] and a Cl-H σ bond orbital was observed at about 4 eV below the main Cl $K\beta_1$ lone pair peak. However, since HCl is a strong acid, one would not expect strong Cl-H bonding at the pH range (4–10) in which the Cl^- (aq) spectrum was measured. Thus one would not expect to observe a peak associated with a H-Cl σ bond unless measurements were made on very acidic solutions. The Cl-H aqueous bond is thus very weak with very little Cl-H σ bonding. This result is consistent with the relatively large Cl-H bond distance obtained by Narten, Vaslow, and Levy [12]. Nevertheless, the Cl $K\alpha$ peak asymmetry and DV- $X\alpha$ calculations suggest localization of the Cl anion is intermediate, lying between the ionic NaCl(s) Cl^- anion and the covalent ClO_4^- anion. If the Cl^- anion were free in the sense that there were no interaction between the anion and the solvent molecules, one would expect a localization similar to NaCl(s). The absence of a Cl-H σ bond suggests localization changes in solution can take place with very little covalent bond overlap. Clearly more theoretical work needs to be done to clarify the detailed nature of solute-solvent chemical interactions in aqueous solution. Finally, no significant Cl-O bonding through the H atom was observed. If such bonding were to take place, a peak at approximately 14 eV below the main Cl $K\beta$ peak would be observed [see the ClO_4^- (aq) Cl $K\beta$ spectra].

The Cl $K\alpha$ and β aqueous spectra were obtained under a range of concentrations [(0.25–0.75) X_s , where X_s is the solute saturation concentration in water] and pH values (4–10) and were obtained by dissolving a number of different solid containing chlorides (e.g., NaCl, LiCl, AlCl_3 , KCl, etc.) in water. In all cases, with the exception of ZnCl_2 and FeCl_3 , systems which are known to exhibit long-range order in solution [9,29], the aqueous Cl $K\beta$ spectra were identical, indicating that Cl^- (aq) can be considered “free” in the sense that there is no intermediate- or long-range ordering around the Cl^- anion in solution.

The Cl $K\alpha$ ($\text{Cl } 1s^{-1}2p^{-1}$) spectra for NaCl(s), Cl^- (aq), and ClO_4^- (aq) are shown in Fig. 2 with the Cl $K\alpha$ peak asymmetry increasing as one moves from ClO_4^- (aq) to NaCl(s). Again, one can see that the intensity in the high-energy region of the main peak increases with ionicity. Since Cl $K\alpha$ is an inner core transition, spectral changes can be attributed to multiple ionization or secondary effects and cannot be directly attributed to changes in the valence electron structure [15]. This greatly simplifies the spectral interpretation and confirms the Cl $K\beta$ spectral observations. Kawai and co-workers have studied the Cl $K\alpha$ high-energy asymmetry as a function of ionicity [15,25–27]. Their results are consistent with our results. Furthermore, based on theoretical DV- $X\alpha$ calculations, the unresolved Cl $K\alpha''$ (“parasitic” satellite) peak was assigned to multiple-

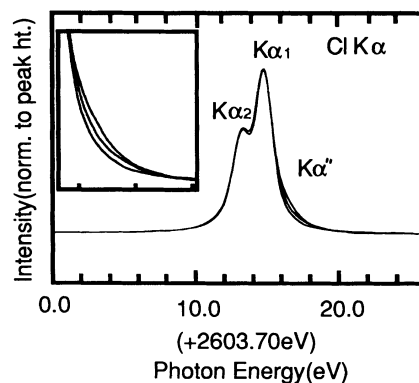


FIG. 2. The Cl $K\alpha$ spectra are plotted for NaCl(s), Cl^- (aq), and ClO_4^- (aq), where the relatively narrow spectra corresponds to Cl^- (aq). The Cl $K\alpha''$ region is expanded and plotted in the upper left of the figure as an aid in visualizing the spectral asymmetry differences between the three Cl species. Cl $K\alpha_1$ and $K\alpha_2$ are assigned to $\text{Cl } 1s^{-1}2p_{3/2}^{-1}$ and $\text{Cl } 1s^{-1}2p_{1/2}^{-1}$ spin-orbit-split transitions, respectively.

ionization transitions similar to those observed for the Cl $K\beta$ peak [15]. Thus we can say that the changes in the Cl $K\beta$ spectra are primarily not intrinsic changes in the valence band, but involve changes in the localization or ionicity of the Cl^- nearest-neighbor bond that affects the Cl^- valence electron shakeoff probability.

Aqueous sulfide solutions were also investigated as well. In Fig. 3, S^{2-} (aq), SH^- (aq), and Na_2S (s) spectra are plotted. The first aspect that deserves attention is that the SH^- (aq) and S^{2-} (aq) spectra are similar and probably representative of a SH^- species since H_2S is a weak acid and appreciable S-H coordination can be expected at normal pH values [30]. The second point is that in contrast to the chloride system, a σ bonding peak is observed at approximately 3.5 eV below the S lone pair

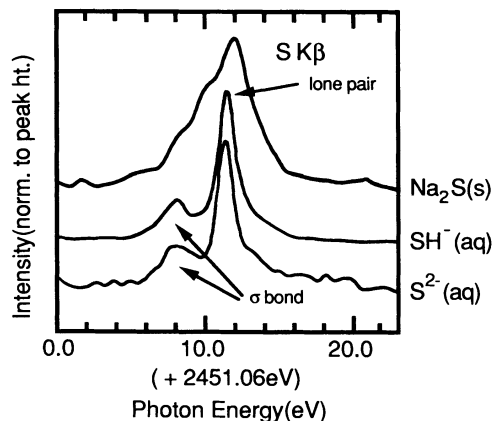


FIG. 3. The S $K\beta$ spectra are plotted for S^{2-} (aq), SH^- (aq), and Na_2S (s). In contrast to the Cl $K\beta$ aqueous spectra, a peak on the low-energy side of the main lone pair peak, which is assigned to the S-H σ bonding orbital, is observed.

peak and is another indication of strong S-H coordination. The presence of a S-H σ bond for sulfide solutions is in contrast to the absence of any Cl-H σ bond, but is not surprising based on the relative acid strength of HCl (complete disassociation) relative to H₂S or SH⁻. An additional point is that the FWHM of the Cl $K\beta$ main peak and the S $K\beta$ main peak are nearly the same with the small differences attributed to instrumental broadening [31]. Since the SH⁻(aq) and S²⁻(aq) S $K\beta$ sulfide spectra were independent of sulfide concentration, the SH⁻(aq) and S²⁻(aq) S $K\beta$ spectra are believed to be representative of a free SH⁻ species with no long-range order. There is also a high-energy asymmetry which is similar to that observed for Cl⁻(aq). Since the nearest neighbor of the emitting atom is the same (H) for both Cl⁻(aq) and S²⁻(aq), one expects a similar multiple-ionization or shakeoff probability since the ionicity of the Cl nearest-neighbor bond is nearly the same.

In conclusion, HRXRFS has been introduced as a tool that can be used to selectively probe the valence density of states of atoms in solution in a unique way that cannot be provided by other techniques. In particular, the chloride investigation shows large spectral changes in the Cl $K\beta$ and Cl $K\alpha$ spectra that can be interpreted as being due to changes in the localization of the Cl nearest-neighbor bond as NaCl(s) is dissolved in water. Further, the Cl $K\beta$ spectra reveal very little Cl-H σ bonding and essentially no Cl-O bonding, suggesting changes in the localization of the Cl⁻ anion can take place with very little covalent bonding between Cl⁻ and H. The sulfide study shows that in contrast to Cl⁻(aq), S²⁻ coordinates rather strongly to H in water and as a result a strong S-H covalent peak is observed nearly 3.5 eV below the main S $K\beta_1$ lone pair peak. This observation is also consistent with the strong acidic nature of HCl relative to H₂S.

One of us (T.S.) would like to thank the Japanese Society for the Promotion of Science for financial support. The assistance of Dr. Sei Fukushima is greatly appreciated.

-
- [1] A. Meisel, G. Leonhardt, and R. Szargan, *X-Ray Spectra and Chemical Binding*, Springer Series in Chemical Physics Vol. 37 (Springer-Verlag, Berlin, 1989).
 - [2] J. A. Catterall and J. Trotter, *Philos. Mag.* **8**, 897 (1963).
 - [3] D. W. Fischer and W. L. Baun, *Phys. Rev.* **138**, A1047 (1965).
 - [4] K. B. Garg and E. Kallne, *Phys. Status Solidi (b)* **70**, K121 (1975).
 - [5] C. F. Hague, C. Senemaud, and H. Ostrowiecki, *J. Phys. F* **10**, L267 (1980).
 - [6] G. Andermann and H. C. Whitehead, *Adv. X-Ray Anal.* **14**, 453 (1971).

- [7] While core levels do experience energy shifts in response to charge transfer in the valence state, these energy shifts are not important in our discussion since the spectral profile changes are of primary interest here. Furthermore, core energy shifts are to a great extent offset by similar energy shifts in the valence band.
- [8] R. D. Deslattes, *Phys. Rev.* **133**, A390 (1964); **133**, A399 (1964).
- [9] K. G. Dyall and R. E. LaVilla, *Phys. Rev. A* **34**, 5123 (1986).
- [10] R. D. Deslattes, R. E. LaVilla, P. L. Cowan, and A. Henins, *Phys. Rev. A* **27**, 27 (1983).
- [11] J. Kawai, C. Satoko, K. Fujisawa, and Y. Gohshi, *Phys. Rev. Lett.* **57**, 988 (1986).
- [12] A. H. Narten, F. Vaslow, and H. A. Levy, *J. Chem. Phys.* **58**, 5017 (1973).
- [13] A. Fontaine, P. Lagarde, D. Raoux, M. P. Fontana, G. Maisano, P. Migliardo, and F. Wanderlingh, *Phys. Rev. Lett.* **41**, 504 (1978).
- [14] E. Matsubara and Y. Waseda, *J. Phys. Condens. Matter* **1**, 8575 (1989).
- [15] H. Siegbahn, *J. Phys. Chem.* **89**, 897 (1985).
- [16] Y. Gohshi, H. Kamade, K. Kohra, T. Utaka, and T. Arai, *Appl. Spec.* **36**, 171 (1982).
- [17] A. Savitzky and M. J. E. Golay, *Anal. Chem.* **36**, 1627 (1964).
- [18] S. Muramatsu and C. Sugiura, *Phys. Rev. B* **27**, 3806 (1983).
- [19] C. Sugiura, *Phys. Rev. B* **9**, 2679 (1974).
- [20] While the most recent multiple-ionization assignments have been made for Ar $K\beta$, it can be argued that the assignments will not significantly change since Cl⁻ and Ar are isoelectronic. See Refs. [18] and [19].
- [21] There are essentially no Cl $K\beta$ spectral differences between undamaged NaClO₄(s) and ClO₄⁻(aq). This is reasonable since the ClO₄⁻ anion is retained even when NaClO₄(s) is dissolved in water.
- [22] T. Åberg, *Phys. Rev.* **156**, 156 (1967).
- [23] L. Pauling, *The Nature of the Chemical Bond* (Cornell Univ. Press, Ithaca, NY, 1960), 3rd ed., p. 93.
- [24] C. Satoko, M. Tsukada, and H. Adachi, *J. Phys. Soc. Jpn.* **45**, 1333 (1978).
- [25] J. Kawai, K. Fujisawa, Y. Gohshi, and C. Satoko, *Spec. Acta* **42B**, 729 (1987).
- [26] J. Kawai, K. Fujisawa, Y. Gohshi, and C. Satoko, *Spec. Acta* **42B**, 745 (1987).
- [27] J. Kawai, C. Satoko, and Y. Gohshi, *Spec. Acta*, **42B**, 1125 (1987).
- [28] E. Gilberg, *Z. Phys.* **236**, 21 (1970).
- [29] M. Magini and T. Radnai, *J. Chem. Phys.* **71**, 4255 (1975).
- [30] F. A. Cotton and G. Wilkinson, *Advanced Inorganic Chemistry* (Wiley, New York, 1988), 5th ed., p. 501.
- [31] This can be easily understood by differentiating Bragg's law ($n\lambda = 2d \sin\theta$). By doing so, one obtains the following expression: $R = \lambda/d\lambda = \tan\theta$. Thus, as θ increases (lower photon energy), the resolving power (R), or, in other words, the energy resolution, improves.